0.80 mol) were added and the mixture was stirred for 30 min at room temperature. $DBADH_2$ (4.60 g, 20 mmol) and *p*-chlorobenzyl alcohol (57.0 g, 0.40 mol) were added successively, and the mixture was heated for 1.5 hours on an oil-bath between 80° to 90°C while O_2 was gently bubbled through the reaction mixture. After cooling to room temperature, the mixture was diluted by addition of Et_2O (500 ml; Et, ethyl) and filtered through a pad of Celite. The solution was washed successively with water (200 ml), 1 M HCl (200 ml), and 200 ml of saturated aqueous NaCl solution, dried over $MgSO_4$, and evaporated in vacuo. The resulting residue was distilled (boiling point between 95° and 98°C, 18 torr) to afford 46.5 g (83%) of *p*-chlorobenzaldehyde. ^1H nuclear magnetic resonance (NMR) ($CDCl_3$, 300 MHz) δ_H 9.98 (1H, s), 7.82 (2H, d, coupling constant J = 8.4 Hz), 7.50 (2H, d, J = 8.4 Hz). ^{13}C NMR ($CDCl_3$, 75.5 MHz) δ_C 191.3, 141.5, 135.4, 131.5, and 130.0.

18. Dedicated to the memory of Zdenek Janousek. Financial support of this work was provided by Zeneca Limited, through the Zeneca Strategic Research Fund. I.E.M. is grateful to Zeneca for receiving the Zeneca Fellowship (1994–1997).

10 September 1996; accepted 31 October 1996

Formation of Chiral Interdigitated Multilayers at the Air-Liquid Interface Through Acid-Base Interactions

Ivan Kuzmenko, Ronith Buller, Wim G. Bouwman, Kristian Kjær, Jens Als-Nielsen, Meir Lahav, Leslie Leiserowitz*

Thin interdigitated films composed of a long-chain, water-insoluble chiral acid (*p*-pentadecylmandelic acid of absolute configuration *R*) and a water-soluble chiral base (phenylethylamine, *R′*) were constructed at the air-solution interface. The (*R, R′*) structure was characterized to near-atomic resolution by grazing-incidence x-ray diffraction (GIXD). The two diastereomeric systems, (*R, R′*) and (*R, S′*), demonstrate similar surface pressure–molecular area isotherms, but their structures are completely different on the molecular level, as monitored by GIXD. Complementary data on these two architectures were provided by atomic force microscopy.

An important goal of supramolecular chemistry is to find methods to control and stabilize the assembly of molecules into larger structures. One approach is to use the air-solution interface to regulate the assembly process by incorporating strong directional interactions for the generation of ultrathin films. The formation of multilayer films from long-chain molecules with polar head groups by the Langmuir-Blodgett (LB) method is straightforward, but the films must be transferred to a substrate and are not especially stable even after transfer. Such a formation process is governed by relatively weak hydrophobic and hydrophilic interactions.

We have considered the effect of using stronger acid-base interactions to control assembly and have constructed an interdigitated film at the air-solution interface akin to that of a natural membrane (*1*). We did this by spreading a water-insoluble, long-chain acid on an aqueous solution containing the complementary amine. Compression of the film causes alternating acid-base groups to emerge at either side of the membrane, whereas the central part contains the interdigitated hydrophobic groups of the acid in space-filling contact across a central plane (Scheme 1). Both the acidic (A) and basic (B) head groups are attached to a chiral carbon center, and the layering and ordering in these films differ greatly between acids and bases of the same handedness (*R, R′*) versus opposite handedness (*R, S′*). The major tool applied for structure elucidation was grazing-incidence x-ray diffraction (GIXD), which allowed us to probe the molecular packing arrangements of the crystalline film to near-atomic resolution.

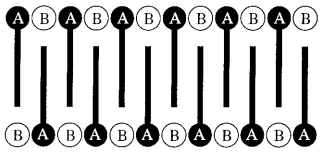

Scheme 1.

In a search for an appropriate bimolecular system that satisfied the above criteria, we came across the crystal structures of diastereomeric phenylethylamine mandelates (*2, 3*). The structure composed of phenylethylamine (PEA) and mandelic acid (MA) molecules of the same handedness, either (*R, R′*) or (*S, S′*), is characterized by rigid hydrogen-bonded bilayers (Fig. 1A). The phenyl rings within each layer are oriented and positioned in a way that is compatible with the formation of an interdigitated arrangement as in Scheme 1, where only the phenyl ring of the mandelic acid is modified by attaching a long hydrocarbon chain in the para position.

The surface pressure–molecular area (π-A) isotherms of (*R*)-pentadecylmandelic acid [*p*-$C_{15}H_{31}$–C_6H_4–CH(OH)COOH (C_{15}-MA) (*4*)] were measured on Millipore-filtered water and on aqueous 0.008 M solutions of (*R*)- and of (*S*)-PEA (C_6H_5–$CHCH_3NH_2$) (Fig. 2A). The isotherm on water demonstrated regular behavior with an extrapolated A of 24 to 25 Å^2. The isotherms for the solutions of two PEA enantiomers have peculiar but similar shapes. Both isotherms are expanded and reach a plateau at $A \sim 40$ Å^2 and π = 42 to 43

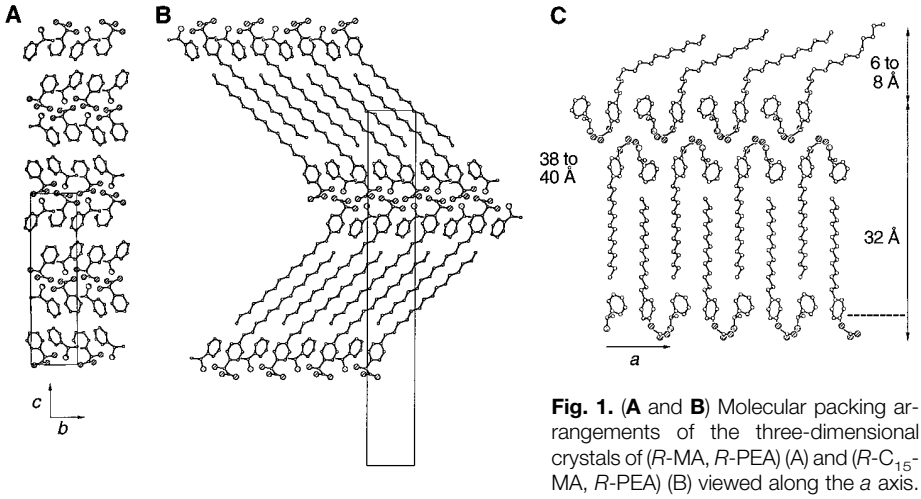

Fig. 1. (**A** and **B**) Molecular packing arrangements of the three-dimensional crystals of (*R*-MA, *R*-PEA) (A) and (*R*-C_{15}-MA, *R*-PEA) (B) viewed along the *a* axis. (**C**) Packing arrangement of the interdigitated (*R*-C_{15}-MA, *R*-PEA) trilayer viewed along the *b* axis. The amorphous and crystalline parts are indicated by the upper and lower arrows at the right; the dashed line represents the air-water interface.

I. Kuzmenko, R. Buller, M. Lahav, L. Leiserowitz, Department of Materials and Interfaces, Weizmann Institute of Science, Rehovot 76100, Israel.
W. G. Bouwman and K. Kjær, Department of Solid State Physics, Risø National Laboratory, DK-4000 Roskilde, Denmark.
J. Als-Nielsen, Niels Bohr Institute, H. C. Ørsted Laboratory, DK-2100 Copenhagen, Denmark.

*To whom correspondence should be addressed.

mN/m (5). The kink preceding the plateau region appears to be sharper for the amphiphile and solute molecules of the same handedness. A pronounced difference between the two isotherms exists in the region of low A. The isotherm for the (*R*, *R*′) system displays a second rise in the π-*A* curve at $A \approx 13$ Å^2, whereas the plateau for the (*R*, *S*′) system extends to the end of the isotherm measured.

No GIXD peaks were observed for both diastereomeric systems (6) at two points along their isotherms, $A = 60$ and 50 Å^2, corresponding to the expanded region before the plateau. Further compression to $A = 30$ Å^2, corresponding to a point on the plateau, gave rise to a strong diffraction signal only for the (*R*, *R*′) system (Fig. 2B). Five observed reflections were indexed for a rectangular cell with $a = 8.32$ Å and $b = 6.82$ Å. From the width of the Bragg rods (7, 8) we estimated the thickness of the crystalline layer to be 32 to 35 Å (Fig. 2, C to G). The (*R*, *S*′) system did not diffract at the same point of the isotherm ($A = 30$ Å^2), nor did it diffract on further compression to a molecular area of $A = 20$ Å^2.

Complementary information on the thickness of the (*R*, *R*′) and (*R*, *S*′) films was obtained by atomic force microscopy (AFM) (Fig. 3, A and C, respectively) (9). The films were transferred in a compressed state at $A = 20$ Å^2 onto mica by the LB technique (10). The (*R*, *R*′) film consisted of patches with two typical heights, 15(2) and 38(4) Å (numbers in parentheses are standard errors in the last digit). Friction-type measurements had shown that the surfaces at both heights are hydrophobic (they have the same friction coefficient, which is smaller than that of mica) (Fig. 3B) (11). The (*R*, *S*′) sample consisted of layers with two typical heights, 16(2) and 32(4) Å. According to the friction-type measurements, the surface at 16(2) Å appears to be hydrophobic, whereas the surface at 32(4) Å demonstrates friction values almost as high as for mica, indicating a hydrophilic character (Fig. 3D).

The GIXD and AFM data suggested the formation of an interdigitated molecular arrangement for the (*R*, *R*′) film at the air-liquid interface. We thus anticipated a similar motif for the corresponding macroscopic crystal. A single crystal of (*R*-C_{15}-MA, *R*-PEA), grown from tetrahydrofuran solution, was subjected to an x-ray structure analysis (12). The crystal has orthorhombic symmetry [space group $P2_12_12_1$, $a = 8.347(1)$ Å, $b = 6.864(2)$ Å, $c = 51.84(1)$ Å, Z (number of formula units per cell) = 4] (Fig. 1B). The head groups [–C_6H_4–CH(OH)COO^- and C_6H_5–$CH(CH_3)NH_3^+$] form hydrogen-bonded bilayers, as in the analogous crystalline complex (*R*-MA, *R*-PEA). The packing incompatibility between alternating C_{15}-MA and unsubstituted PEA molecular ions within a layer is compensated by interdigitation of the hydrocarbon chains from neighboring bilayers related by twofold screw symmetry along the *a* axis.

The match in lattice dimensions of the crystalline thin films of (*R*-C_{15}-MA, *S*-PEA) on the liquid surface to those of the corresponding three-dimensional (3D) crystal structure and the thickness of the crys-

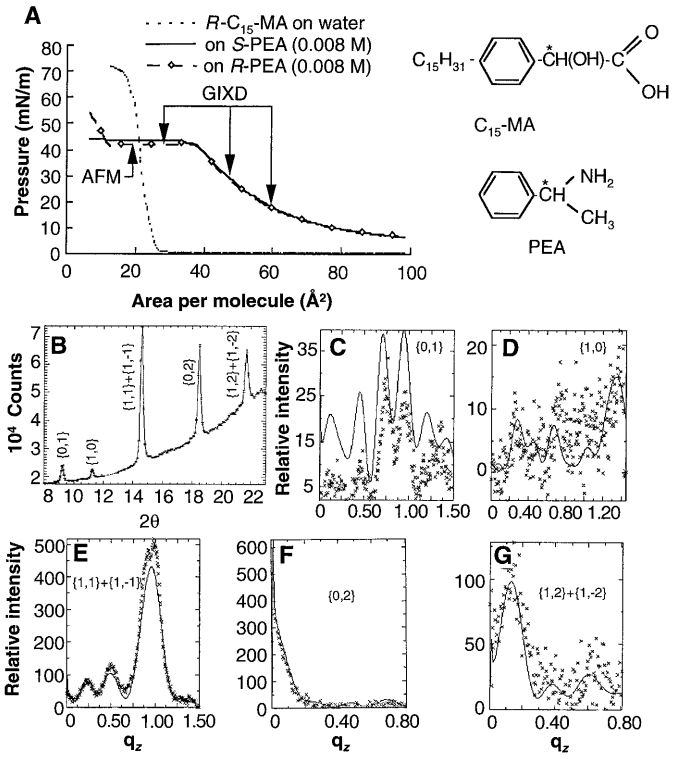

Fig. 2 (**left**). (**A**) Surface pressure–area (π-*A*) isotherms of *R*-C_{15}-MA on Millipore water and PEA aqueous solutions. The arrows show the states at which GIXD patterns were recorded and AFM measurements for the corresponding LB films were performed. (**B** through **G**) The GIXD pattern of *R*-C_{15}-MA spread over 0.008 M aqueous solution of *R*-PEA and compressed to an area $A = 30$ Å^2 per molecule at a temperature of 5°C. Shown in (B) are the observed GIXD Bragg peaks with assigned (*h*,*k*) indices, where 2θ corresponds to the $\mathbf{q}_{xy}$ in-plane component of the wave vector **q** (wavelength $\lambda = 1.339$ Å). The corresponding measured (crosses) and calculated (solid line) Bragg rod intensity profiles in (C) through (G) are based on the molecular model described in the text; $\mathbf{q}_z$ is the out-of-plane component of the wave vector **q** in units of Å^{-1}.

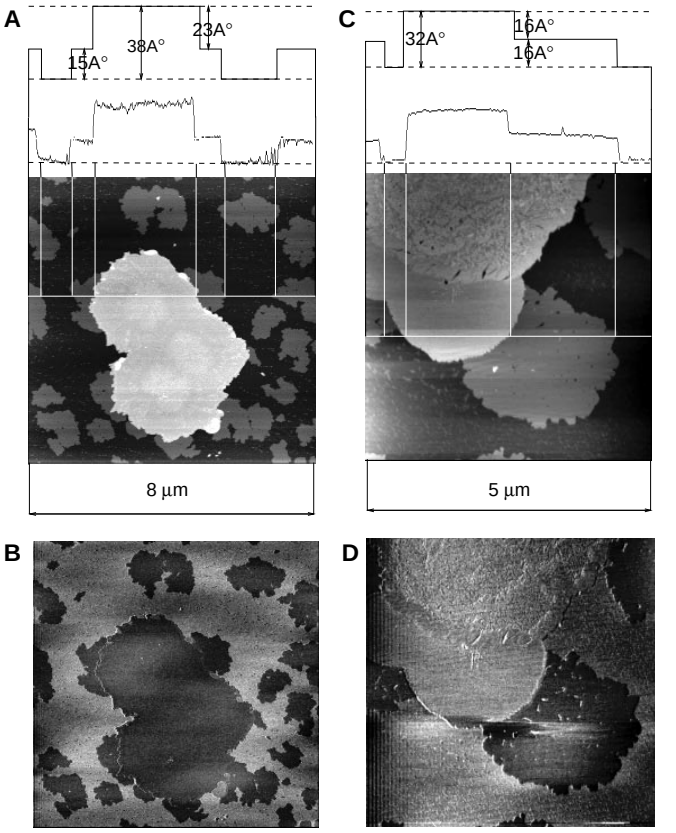

Fig. 3 (**right**). AFM images and the corresponding height profiles of the (*R*-C_{15}-MA, *R*-PEA) and (*R*-C_{15}-MA, *S*-PEA) films transferred onto mica by the LB technique at a molecular area $A = 30$ Å^2 per molecule and surface pressure $\pi \approx 40$ mN/m: topography (**A**) and friction-force map (**B**) for (*R*-C_{15}-MA, *R*-PEA); topography (**C**) and friction-force map (**D**) for (*R*-C_{15}-MA, *S*-PEA). The vertical lines are a guide for the eye.

talline part of the films, as determined from the Bragg rod widths together with AFM height and friction analysis, indicated formation of a composite trilayer in the plateau region of the isotherm (Fig. 1C). This film consists of a crystalline interdigitated bilayer as in the corresponding 3D crystal structure and a partially disordered monolayer on the top. This monolayer is crystalline at the level of the MA and PEA units by virtue of the hydrogen-bonding bilayer network and is disordered on the top level of the alkyl chains because of the gaps created by the interleaved PEA units (*13*). This molecular model (*14*) proved to be most satisfactory, fitting the observed GIXD data well (Fig. 2, C to G). The one noticeable misfit in scale between the observed and calculated (0,1) Bragg rods arises from beam damage of the sample during the GIXD measurements (*15*).

In terms of molecular reorganization, the absence of diffraction in the first part of the π-*A* isotherm before the plateau can be attributed to incompatibility between the C_{15}-MA and PEA molecules: when the latter are incorporated in the monolayer, they create gaps between C_{15}-hydrocarbon chains. This alternating juxtaposition does not permit close packing and crystalline organization of the monolayer. The plateau region of the isotherm at 13 Å^2 < *A* < 40 Å^2 per molecule for *R*-C_{15}-MA spread on *R*-PEA solution reflects a phase transition corresponding to the gradual transformation of the amorphous monolayer into the composite interdigitated trilayer. The second rise of the surface pressure at 13 Å^2 per molecule reflects a higher compressibility of the trilayer phase that should completely cover the liquid surface at this area (this estimate is based on the cell dimensions of the crystalline film). In Scheme 2A we suggest a simple mechanism for the formation of such a trilayer. We assume that the crystallization starts at the folding stage by virtue of the formation of a stable hydrogen-bonded bilayer, which is maintained upon further compression, leading to an interdigitated trilayer.

The process of molecular reorganization along the isotherm for the (*R*, *S′*) system is less well understood. Our explanation relies primarily on the AFM analysis and the absence of diffraction in the GIXD measurements. The two typical heights of 16(2) Å (hydrophobic surface) and 32(3) Å (hydrophilic surface) suggest that, after the kink at ~40 Å^2 per molecule, the disordered monolayer transforms into an amorphous bilayer. We speculate how it may be generated in Scheme 2B, assuming that the bilayer at the folding stage is much less stable and is presumably disrupted upon further compression. We propose that the contrast in structural rearrangements of the (*R*-C_{15}-MA, *R*-PEA) and (*R*-C_{15}-MA, *S*-PEA) films on compression arises from the different energies of the hydrophilic bilayer of the head groups at the folding stage as in Scheme 2, and we believe that this contrast correlates with the drastic differences in solubility, crystallization behavior, and heats of fusion (12.4 and 6.6 kcal/mol) (*16*) of their two water-soluble diastereomeric analogs, (*R*-MA, *R*-PEA) and (*R*-MA, *S*-PEA), respectively. Although for both diastereomeric crystals the overall hydrogen-bonding arrangements are similar (*3*, *17*), the orientations and positions of the phenyl rings within a layer in the (*R*-MA, *S*-PEA) salt are not compatible with the formation of an interdigitated structure (*18*).

GIXD experiments with chiral *R*-C_{15}-MA on a racemic solution of PEA yielded a diffraction pattern similar to that obtained for the (*R*-C_{15}-MA, *R*-PEA) system, but with Bragg peaks of reduced intensity and increased width, showing formation of fewer trilayer crystallites of smaller size. This result arises from the chiral discrimination involving a separation of (*R*) and (*S*) enantiomers of PEA at the solution interface. On the other hand, GIXD experiments on a racemic C_{15}-MA monolayer, which demonstrated a π-*A* isotherm similar to that obtained for the (*R*, *S′*) system over a chiral or racemic PEA solution, did not yield diffraction signals, suggesting that the long-chain amphiphilic molecules did not separate into islands of opposite chirality.

We believe that the proposed approach for the molecular design of thin interdigitated films can be extended to other two-component systems composed of a water-insoluble amphiphile and a water-soluble counterpart. Moreover, the ability of such systems to form stable bilayers at the air-liquid interface, and thus to be amenable to characterization at the near-atomic level, may enable us to probe the mechanism of ion transport that occurs in natural membranes.

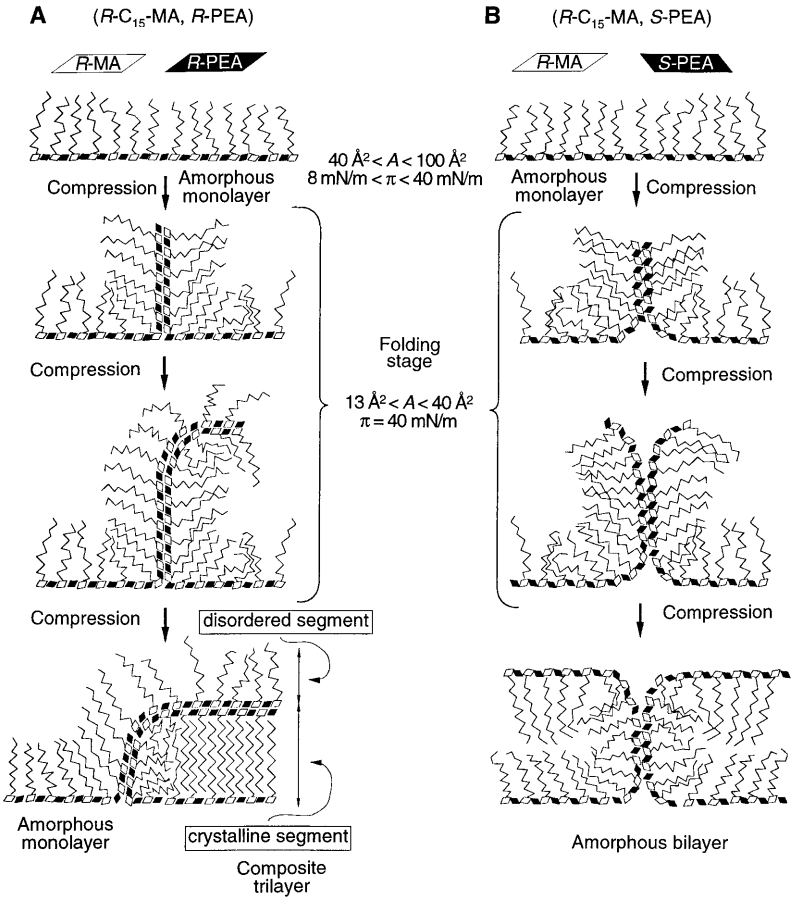

Scheme 2.

REFERENCES AND NOTES

1. J. L. Slater and C. H. Huang, *Prog. Lipid Res.* **27**, 325 (1988).
2. M. C. Brianso, M. Leclercq, J. Jacques, *Acta Crystallogr.* **B35**, 2751 (1979).
3. S. Larsen and H. L. Diego, *ibid.* **B49**, 303 (1993).
4. We synthesized (*R*)-*p*-pentadecylmandelic acid by the Friedel-Craft reaction of pentadecyl benzene with oxalyl chloride in chloroform at 0° to 5°C to yield the α-keto acid [O. Itoh *et al.*, *Bull. Chem. Soc. Jpn.* **57**, 810 (1984)]. The latter was esterified to the corresponding methoxy ester and subsequently reduced by the $NaBH_4$ (*R*, *R*)tartaric acid complex according to the method of H. Iwagami *et al.* [*ibid.* **64**, 175 (1991)] to yield (*R*)-*p*-pentadecyl methyl mandelate with an enantiomeric excess (ee) of 57%. We determined this value by nuclear magnetic resonance

(NMR) analysis, using the *tris*[3-(trifluoromethylhydroxymethylene)-(+)camphorato]europium(III) complex. The compound was hydrolyzed to the corresponding acid and then the optical purity was enhanced up to 97% ee by cocrystallization with commercially available *R*-PEA. The optical purity was checked by NMR and circular dichroism spectra: $[\alpha]_D^{25} = -63.2$ (C = 1.01 g/liter tetrahydrofuran).
5. The isotherms were measured from $A = 100$ to 5 Å^2 per molecule.
6. The GIXD measurements were conducted on a liquid surface diffractometer at the undulator beamline BW1 at HASYLAB, Deutsches Elektronen-Synchrotron (DESY). The synchrotron radiation beam was monochromated to a wavelength of 1.339 Å. The incident angle was adjusted to $\alpha_f = 0.85\alpha_c$, where $\alpha_c \approx 0.14°$. A detailed explanation of the method and experimental setup are given in (*7*) and (*8*), respectively. The amphiphile *R*-C_{15}-MA was spread at room temperature in a Langmuir trough and then cooled to 5°C.
7. J. Als-Nielsen *et al*., *Phys. Rep.* **246**, 251 (1994).
8. J. Majewski, *Chem. Eur. J.* **1**, 304 (1995).
9. We implied, although we have not proven, that no significant changes occurred on deposition of the films on a solid support. The AFM measurements were performed with Nanoscope III FM (Digital Instruments, Goleta, CA) at ambient temperature with a commercial silicon nitride tip, attached to a cantilever with a spring constant of 0.38 N/m.
10. Film depositions were done on a NIMA trough (NIMA Technology, Coventry, UK) at 20°C and at a surface pressure of ~40 mN/m. Film was transferred onto mica at a constant speed of 10 mm/min.
11. For the silicon nitride tip used in the AFM studies, the lateral friction coefficient is qualitatively proportional to the hydrophilicity of the surface. A detailed analysis of different factors influencing the lateral friction for self-assembled monolayers on mica is given in Y. Liu *et al*. [*Langmuir* **12**, 1235 (1996)].
12. Crystallographic measurements were performed on a four-circle Rigaku single-crystal diffractometer with Cu K_α radiation from a 18-kW rotating anode generator. The structure was solved and refined with the use of SHELXL-91 software. The coordinates have been submitted to the Cambridge Crystallographic Database.
13. Subtraction of a 25 Å thickness of the crystalline bilayer as in the 3D structure from the 38(4) Å trilayer thickness obtained by AFM leaves 13(4) Å, which is compatible within a standard deviation with the 16(2) Å monolayer thickness.
14. Comparison of the observed and calculated Bragg rods (the latter obtained by x-ray structure factor computations) showed that the alkyl chains on the top level of the trilayer are disordered and there is no ordered binding of PEA from the subphase.
15. Beam damage had in fact occurred, but we lacked the quantitative data to introduce a proper correction.
16. S. P. Zingg, E. M. Arnett, A. T. McPhail, A. A. Bothner-By, W. R. Gilkerson, *J. Am. Chem. Soc.* **110**, 1565 (1988).
17. H. L. Diego, *Acta Chem. Scand.* **48**, 306 (1994).
18. In the complex (*R*-MA, *R*-PEA) the phenyl rings within a layer are uniformly tilted in a manner compatible with close packing of the hydrocarbon chains; in the (*R*-MA, *S*-PEA) salt the phenyl rings are not uniformly tilted.
19. We thank S. Matlis for performing the AFM measurements. Supported by the Minerva Foundation, the German Israeli Foundation (GIF), the Danish Foundation for Natural Sciences, and HASYLAB, DESY, Hamburg, Germany (beam time).

15 July 1996; accepted 8 October 1996

Design of Nonionic Surfactants for Supercritical Carbon Dioxide

J. B. McClain, D. E. Betts, D. A. Canelas, E. T. Samulski, J. M. DeSimone,* J. D. Londono, H. D. Cochran, G. D. Wignall,* D. Chillura-Martino, R. Triolo

Interfacially active block copolymer amphiphiles have been synthesized and their self-assembly into micelles in supercritical carbon dioxide (CO_2) has been demonstrated with small-angle neutron scattering (SANS). These materials establish the design criteria for molecularly engineered surfactants that can stabilize and disperse otherwise insoluble matter into a CO_2 continuous phase. Polystyrene-*b*-poly(1,1-dihydroperfluorooctyl acrylate) copolymers self-assembled into polydisperse core-shell–type micelles as a result of the disparate solubility characteristics of the different block segments in CO_2. These nonionic surfactants for CO_2 were shown by SANS to be capable of emulsifying up to 20 percent by weight of a CO_2-insoluble hydrocarbon into CO_2. This result demonstrates the efficacy of surfactant-modified CO_2 in reducing the large volumes of organic and halogenated solvent waste streams released into our environment by solvent-intensive manufacturing and process industries.

More than 30 billion pounds of organic and halogenated solvents are used worldwide each year as process aids, cleaning agents, and dispersants (*1*), and solvent-intensive industries are considering alternatives that can reduce or eliminate the negative impact that solvent emissions can have on the environment. Because of its low cost, wide availability, and environmentally and chemically benign nature (*2*, *3*), CO_2 is an attractive solvent alternative for a wide variety of chemical and industrial processes. Although CO_2, in both its liquid and supercritical (sc) states, readily dissolves many small molecules (*4*), it is a very poor solvent—at easily accessible conditions (temperature <100°C and pressure <300 bar)—for many substances, and commercial applications of pure CO_2 as a solvent have been infrequent. Materials that have disappointingly low solubilities in pure CO_2 include most polymers [except amorphous or low-melting fluoropolymers and silicones (*2*, *4*, *5*)], waxes, heavy oils, machine-cutting fluids, solder fluxes, photoresists, proteins, salts, and metal oxides. The design and characterization of surfactants that enhance the solubilizing properties of CO_2 is therefore crucial for its widespread application.

Block and graft copolymers composed of chain segments with dissimilar solubility characteristics self-assemble into well-defined structures when placed in a medium that is a good solvent for one of the segments (the lyophilic segment) and a poor solvent for the other segment (the lyophobic segment) (*6*–*9*). These nonionic surfactants are typified by micelles or more complex aggregates in which the lyophobic segments form a core surrounded by a shell of the highly solvated lyophilic segments that extend into the continuous phase (*6*). The core regions of such micelles are technologically useful, as they are capable of emulsifying otherwise insoluble materials into a microphase-separated environment within a preferred continuous solvent phase (*9*). Here, we report the direct structural characterization by SANS of well-defined, spherical micelles resulting from a series of molecularly engineered block copolymer surfactants in $scCO_2$. Our results also demonstrate the efficacy of these surfactants in emulsifying insoluble solutes into CO_2. This development may ultimately enable surfactant-modified CO_2 to be used as a replacement for conventional solvent systems currently used in manufacturing and service industries, such as precision cleaning (metal finishing, microelectronics, optics, or electroplating), medical device fabrication, and dry (garment) cleaning, as well as in the chemical manufacturing and coating industries.

Several laboratories have demonstrated progress in the micellization of aqueous and polar materials in many dense sc fluids including alkanes, chlorofluorocarbons, hydrofluorocarbons, and CO_2 (*10*–*15*). However, success in designing generic surfactants for CO_2 has been hindered by the challenge of identifying lyophilic segments for CO_2. A promising lead for the design of highly effective surfactants for CO_2 arose out of two related discoveries: (i) that CO_2 is thermodynamically a good solvent for fluorinated acrylate polymers [positive second virial coefficient (*13*, *16*)], and (ii) that these same polymers could be synthesized

J. B. McClain, D. E. Betts, D. A. Canelas, E. T. Samulski, J. M. DeSimone, Department of Chemistry, University of North Carolina, CB 3290, Venable and Kenan Laboratories, Chapel Hill, NC 27599, USA.
J. D. Londono, H. D. Cochran, G. D. Wignall, Oak Ridge National Laboratory, Oak Ridge, TN 37831, USA.
D. Chillura-Martino and R. Triolo, Departimento di Chimica Fisica, University of Palermo, 90123 Palermo, Italy.
*To whom correspondence should be addressed.

Formation of Chiral Interdigitated Multilayers at the Air-Liquid Interface Through Acid-Base Interactions

Ivan Kuzmenko, Ronith Buller, Wim G. Bouwman, Kristian Kjær, Jens Als-Nielsen, Meir Lahav and Leslie Leiserowitz (December 20, 1996)

Science **274** (5295), 2046-2049. [doi: 10.1126/science.274.5295.2046]

Editor's Summary

Science (print ISSN 0036-8075; online ISSN 1095-9203) is published weekly, except the last week in December, by the American Association for the Advancement of Science, 1200 New York Avenue NW, Washington, DC 20005.